AGU100 ADVANCING EARTH AND SPACE SCIENCE

Geochemistry, Geophysics, Geosystems

RESEARCH ARTICLE
10.1029/2018GC007603

Special Section:
FRONTIERS IN GEOSYSTEMS: Deep Earth - surface interactions

Key Points:
- Finite frequency *P* wave tomography images a gap in the subducted lithosphere beneath the eastern Greater Antilles
- This gap is consistent with segmentation tearing from differential rollback and extension
- The presence of microplates may facilitate tearing and deformation in the Caribbean and elsewhere

Supporting Information:
- Figure S1

Correspondence to:
C. W. Harris,
cwharris@usc.edu

Citation:
Harris, C. W., Miller, M. S., & Porritt, R. W. (2018). Tomographic imaging of slab segmentation and deformation in the Greater Antilles. *Geochemistry, Geophysics, Geosystems*, *19*, 2292–2307. https://doi.org/10.1029/2018GC007603

Received 10 APR 2018
Accepted 25 JUN 2018
Accepted article online 26 JUL 2018
Published online 3 AUG 2018

Tomographic Imaging of Slab Segmentation and Deformation in the Greater Antilles

Cooper W. Harris[1], **Meghan S. Miller**[1,2], **and Robert W. Porritt**[3]

[1]Department of Earth Science, University of Southern California, Los Angeles, CA, USA, [2]Research School of Earth Sciences, Australian National University, Canberra, ACT, Australia, [3]Institute for Geophysics, University of Texas at Austin, Austin, TX, USA

Abstract We present a new tomographic *P* wave model of the upper mantle in the east Caribbean region. The model was built using 3-D finite frequency sensitivity kernels and ~20,000 teleseismic *P* and *PP* traveltime residuals from 535 events recorded across 130 broadband seismometers. We observe high-velocity features corresponding to a Caribbean beneath northern South America and an arcuate slab beneath the Lesser and Greater Antilles island arcs. The latter exhibits an along strike gradient in dip with steep edges and a reclined middle, consistent with ongoing slab rollback and collision. We divide the arcuate slab into three sections from two lateral discontinuities. The southern and northern Lesser Antilles sections are separated by a gap ~15°N down to ~200 km. Between Puerto Rico and Hispaniola, another gap down to ~300 km separates the northern Lesser Antilles slab from a narrow slab fragment further east. We relate these discontinuities to the subducted North American-South American plate boundary and a slab segmentation tear, respectively. The northern and southern ends of the Lesser Antilles trench are actively deforming from collision and differential rollback. However, these areas exhibit different styles of lithospheric tearing, as manifest in the morphology of the slab. We infer the contrast in tearing relates to the presence of microplates at the northern boundary of the Caribbean plate. Microplates facilitate block divergence and differential trench retreat/rollback, which drive slab segmentation. These results offer new insight into the tectonics of the Caribbean region and the factors driving lithospheric tearing in slabs generally.

Plain Language Summary We use a regional array of seismic stations and global earthquake data to construct a 3-D model of the top 1,000 km of the Earth's mantle in a subduction zone. We image a subducting slab and observe that the slab is tearing while it sinks. Based on regional tectonic knowledge, we infer that this deformation is related to the presence of microplates near the tear. We believe that microplates facilitate tearing by allowing tectonic blocks to move apart from one another and diverge. This divergence at the surface is accommodated at depth via tearing and slab segmentation.

1. Introduction

Lithospheric tearing and slab rollback are observed at arcuate subduction zones globally and are recognized as fundamental processes in subduction zone evolution (e.g., Govers & Wortel, 2005; Royden, 1993). Slab segmentation occurs when subvertical tears in the downgoing lithosphere subdivide a previously continuous arc, thereby driving changes in plate surface velocities, geometric reorganization of the subduction system, and eventual termination of the arc (e.g., Govers & Wortel, 2005; Millen & Hamburger, 1998). The origin of such tears in various settings has been linked to collision between an arc and buoyant features on the downgoing/incoming plate (Sacks & Secor Jr, 1990), trench-retreat and rollback of narrow slab segments (Schellart, 2005), strong horizontal flow near slabs that have reached the deep transition zone (Faccenna et al., 2004), and along-strike variations in rollback velocity (termed differential rollback), especially at the edges of retreating arcs (Govers & Wortel, 2005). The process of differential rollback ultimately produces tensional forces in the subducted lithosphere, which, due to strain localization within the slab, leads to the development of multiple downdip tears that segment the slab and accommodate along-strike divergence (e.g., Doglioni, 1991; Jolivet et al., 2013).

The destruction of arcuate slabs via Subduction-Transform Edge Propagator (STEP) faults due to ongoing collision and rollback has been observed in the Caribbean as well as other arcuate subduction zones (Govers & Wortel, 2005). Other examples of differential rollback are diverse. For example, in the western

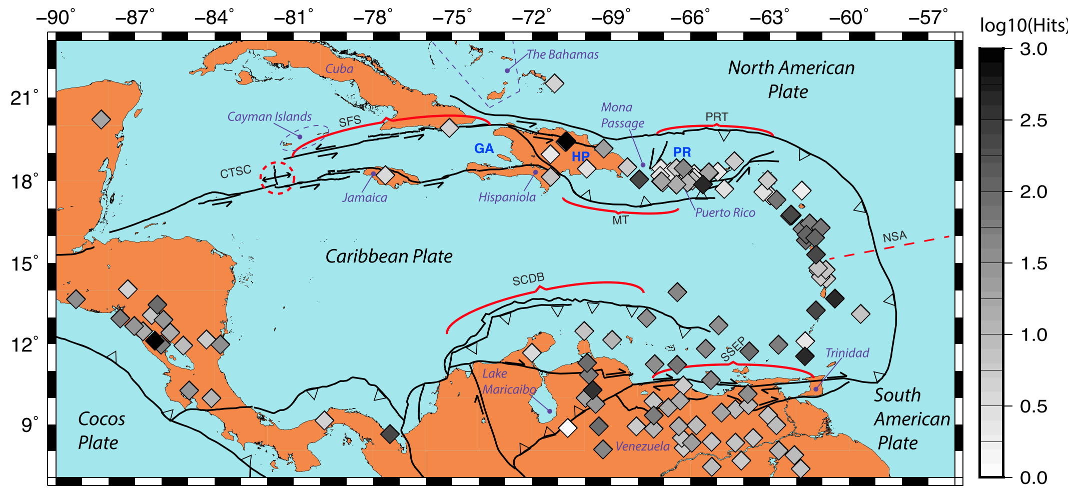

Figure 1. Map of the Caribbean region and seismic station locations. Seismic stations are plotted as diamonds and are shaded to illustrate $\log_{10}$ of data points (hits) used from each station in gray scale. Microplates are labeled in blue font: GA = Gonave microplate; HP = Hispaniola microplate; PR = Puerto Rico microplate. Plate boundary features are labeled in black font and highlighted with red lines: SFS = Septentrional fault system; PRT = Puerto Rico trench; CTSC = Cayman trough spreading center; MT = Muertos trough; NSA = North-South American plate boundary (Gordon, 1998); SCDB = South Caribbean Deformed Belt; SSEP = san Sebastian El Pilar fault system. Geographic features are labeled in indigo. Major faults are plotted as black lines with triangles to indicate convergence direction, half arrows for transform motion, and opposing arrows for divergence (Bird, 2003).

Mediterranean Sea, a slab window has opened north of the Balearic Islands due to radial rollback and the tearing forces of divergence along the arcuate subduction interface (Hinsbergen et al., 2014). In the Tyrrhenian Sea, the slab beneath Italy is observed as a discontinuous feature with multiple segments that have been separated piecewise due to variations in slab rollback rates and multiple collisions of buoyant features with the volcanic arc (Doglioni et al., 1994; Lucente et al., 1999; Rosenbaum et al., 2008). In the Aegean Sea, slab retreat has caused progressive slab tearing, which in turn drove regional extension and strain localization that primed the slab for successive ruptures (Faccenna et al., 2006; Jolivet et al., 2013). Similar examples of segmentation have been detected in the Indian Ocean slab beneath the Andaman Arc (Kumar et al., 2016; Kundu & Gahalaut, 2010), the Hellenic slab beneath Greece (Sachpazi et al., 2016), and the Pacific slab beneath the southern Mariana arc (Miller et al., 2006). In the Marianas and the Calabrian arcs specifically, slab tearing has been related in part to along-strike extension and slab weakening that arise from increased arc curvature and arc-lengthening (Doglioni, 1991; Doglioni, 1995).

Geodynamic models have shown that subduction rollback rates are functions of lower plate buoyancy (e.g., Martinod et al., 2005), subduction velocity of the downgoing plate (e.g., Schellart, 2005), and width of the subducting slab (e.g., Dvorkin et al., 1993). These and other papers predict that narrow, negatively buoyant and slowly subducting slabs will have higher rollback rates than wide, positively buoyant slabs that are subducting more quickly. The Greater Antilles arc, spanning Cuba, the Cayman Islands, Jamaica, Hispaniola, and Puerto Rico, is proximal to a collision between a relic volcanic arc and a buoyant plateau (e.g., Pindell & Kennan, 2009); is characterized by slow, oblique subduction (Calais et al., 1992; Mann et al., 2002); and is experiencing regional extension as identified in GPS data (e.g., Mann et al., 2002; Figure 1). For these reasons, the slab beneath the Greater Antilles may be tearing. In addition, the presence of microplates in the Greater Antilles (e.g., Mann et al., 1995) may have had an unknown effect on slab segmentation. In contrast, a STEP tear has been identified at the southern terminus of the Lesser Antilles volcanic arc, near Trinidad and northern Venezuela (Clark et al., 2008; Govers & Wortel, 2005; Miller et al., 2009; Figure 1).

We investigate the eastern Caribbean region with a new tomographic model constructed with teleseismic *P* wave traveltime residuals and finite-frequency sensitivity kernels. Global inversions (Bijwaard et al., 1998; Taboada et al., 2000; van Benthem et al., 2013), regional passive networks (Bezada et al., 2010; VanDecar et al., 2003), and source-side regional tomography (Van Der Hilst & Mann, 1994) have previously

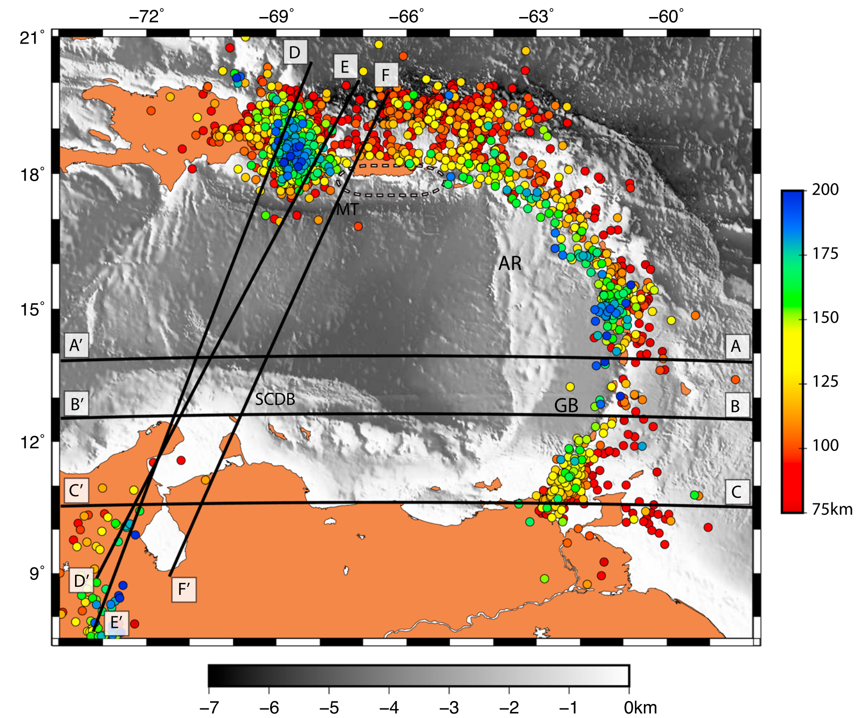

Figure 2. Map of regional bathymetry and intermediate-depth seismicity (70 km ≥ z ≥ 200 km). Epicenters are colored by depth in km. A dashed black and white ellipse represents the lack of intermediate-depth seismicity in the vicinity of Puerto Rico. The solid black lines represent the location of vertical cross-sections through the tomographic model shown in Figures 7 and 8. Bathymetry is colored per the scale beneath the plot. Earthquake data courtesy of the U.S. Geological Survey (USGS). See Figure 1 for labels. Additional bathymetric features are labeled: MT = Muertos trough; AR = Aves ridge; GB = Grenada Basin; SCDB = South Caribbean Deformed Belt.

investigated mantle anomalies in this region. Our new model improves on past efforts through the inclusion of substantially more data, the use of multiple *P* phases, and the use of several overlapping finite frequency measurement bands.

2. Tectonic Setting

The Caribbean plate is located between the North and South American plates and is proposed to have formed in the modern eastern Pacific Ocean during the mid-Cretaceous (Pindell & Dewey, 1982; Pindell & Kennan, 2009; Figure 1). After formation, the Caribbean plate migrated east relative to the North and South American plates (collectively termed the American plates) as Atlantic Ocean lithosphere subducted beneath it (Pindell & Dewey, 1982). During this time, the Great Arc of the Caribbean spanned the length of the plate boundary between the east Caribbean and American plates (Pindell & Kennan, 2009). The arc was volcanically active until the early Eocene (~55 Ma), when the positively buoyant Bahamas Plateau collided with the arc and choked the trench northwest of Hispaniola (Burke, 1988; Pindell & Barrett, 1991; Figure 1). After the collision, three major changes occurred: interplate convergence shifted from being northeast-southwest to predominantly east-west, subduction in the Greater Antilles gave way to oblique collision, and magmatism ceased in the Greater Antilles (Boschman et al., 2014; Perfit et al., 1980; Pindell & Kennan, 2009). This was followed by cessation of volcanism at the Aves Ridge and opening of the Grenada basin as the Caribbean-Atlantic trench retreated, thus forming the modern Lesser Antilles arc (e.g., Aitken et al., 2011; Figure 2).

The collision also led to the formation of the Gonâve, Hispaniola, and Puerto Rico microplates, which sheared off the Caribbean Plate sometime after the Eocene (Mann et al., 1995; Figure 1).

Since forming, these microplates have been translated along bounding faults that divide them from one another and from the Caribbean and North American plates (Byrne et al., 1985; Mann et al., 1995). This

10.1029/2018GC007603

Table 1
Data Table Displaying Total Number of Delay Times Used for P and PP Arrivals in Each Frequency Band (b1-b4)

Phase:	Total delays:	b1: 0.02–0.1 Hz	b2: 0.1–0.4 Hz	b3: 0.4–0.8 Hz	b4: 0.8–2.0 Hz
P	17,491	5,076	4,301	5,136	2,978
PP	1,638	1,166	472	0	0

motion and divergence is a result of ongoing collisional deformation as well as regional gradients in interplate convergence rates (Jansma et al., 2000). The Puerto Rico and Hispaniola microplates are separated by the Mona Passage, a seismically active region that has been interpreted as a zone of intra-arc oblique extension (Chaytor & ten Brink, 2010; Mann et al., 2002; Figure 1). South of the Mona Passage, the Caribbean plate underthrusts the microplates to the north along the roughly east-west Muertos Trough retroarc thrust (Granja Bruña et al., 2009; Figure 1).

The plate boundaries between the Caribbean and North and South American plates are both defined by complex, diffuse zones of transform fault systems (Mann et al., 1990; Silver et al., 1975; Figure 1). Each of these boundaries features a domain of oblique collision in the east that gradationally transitions into regional strike-slip faults further west (Avé Lallemant, 1997; Mann et al., 2002). In the north, there is an east-west transition from volcanic subduction at the northern Lesser Antilles, to amagmatic oblique convergence at the Puerto Rico Trench, to sinistral transform faulting along the $>$1000 km long Septentrional Fault System, to divergence at the Cayman Trough spreading center (Mann et al., 2002; Figure 1). In the south, there is a similar east-west progression from subduction at the southern Lesser Antilles (SLA) to dextral transform faulting along the $>$1,000 km long San Sebastián-El Pilar fault system. Further west, the southern Caribbean plate subducts southward beneath the Maracaibo region of northern South America along the South Caribbean Deformed Belt (Avé Lallemant, 1997; Kellogg & Bonini, 1982). This subduction began sometime around or after the Eocene in order to accommodate convergence between the Caribbean and South American plates (Russo et al., 1993; Speed, 1985).

The South American-Caribbean plate boundary also features an active lithospheric tear at the southernmost Lesser Antilles, near the Gulf of Paria (Clark et al., 2008; Miller et al., 2009; Figure 1). This tear is an example of a downdip STEP fault (Govers & Wortel, 2005), which separates Atlantic oceanic lithosphere subducting westward beneath the Lesser Antilles from the adjacent South American passive margin off the coast of eastern Venezuela, which does not subduct (Clark et al., 2008). Seismically, the tearing has been imaged as taking place south of the Lesser Antilles subduction zone, implying that continental margin lithosphere is subducting along with the oceanic slab (Bezada et al., 2010; Levander et al., 2014).

3. Data and Methods

To investigate upper mantle structure in the eastern Caribbean, we employed finite-frequency *P* wave teleseismic tomography (e.g., Dahlen et al., 2000). Three-dimensional variations in *P* wave velocity may reflect temperature anomalies encountered along or adjacent to raypaths and can be used to infer laterally heterogeneous structure in the mantle, such as subducting lithosphere (e.g: Aki et al., 1977; Humphreys et al., 1984; Nolet, 1987) as well as discontinuities related to the tearing of subducted lithosphere (e.g., Spakman & Wortel, 2004; Wortel & Spakman, 2000). We constructed our final velocity model similarly to the DNA09 (Obrebski et al., 2010; Obrebski et al., 2011) and DNA13 (Porritt et al., 2014) tomographic models of the western and central United States.

Our input data vector consisted of ~20,000 manually measured traveltime residuals, which reflect the difference between observed traveltimes and values predicted using the radially symmetric iasp91global velocity model (Kennett & Engdahl, 1991; Figure S1). Of the residuals, 17,491 were measured from teleseismic *P* waves and 1,638 were measured from teleseismic *PP* waves (Table 1). Data from 483 earthquakes with magnitude $m_w \geq 5.5$ were analyzed, which were recorded across a multinetwork array of 130 broadband stations between 2000 and 2017 (Figure 3 and Table 2).

After picking *P* and *PP* phase arrivals, we employed a multichannel cross-correlation technique (VanDecar & Crosson, 1990) to refine the manual measurements and produce optimized residuals in four nonoverlapping frequency bands (Table 1). This technique utilizes waveform similarity across a network to produce accurate relative arrival times, but information about the absolute traveltime is lost. Only optimized residuals with a cross-correlation coefficient $\geq$ 0.8 were used in the inversion (Figure S1). In finite-frequency tomography, the sensitivity of each traveling seismic wave to voxels in a mesh is approximated as a 3-D Fréchet differential kernel, that is, a hollow, tapering cylinder that extends from a given hypocenter to a given seismometer (Zhao et al., 2000). The width of each such kernel is a function of, among other variables, the frequency band the

10.1029/2018GC007603

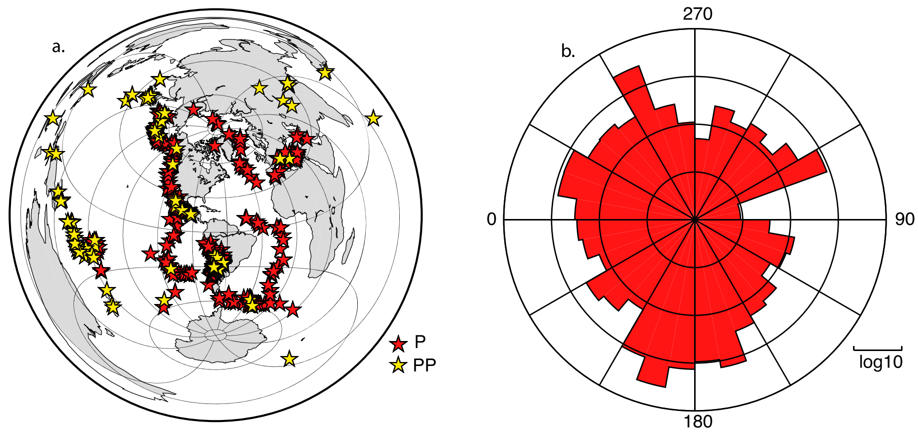

Figure 3. (a) Map of epicenters of all earthquakes used in this study centered on the Caribbean. Events that contributed *P* arrivals to the data set are plotted in red. Events that produced PP arrivals are plotted in yellow. (b) Rose diagram of back azimuthal coverage, measured between station, and event pairs, binned every 10° and plotted as $\log_{10}$ of the totals.

kernel is calculated in and the assumed 1-D structure along the raypath (Hung et al., 2000). Therefore, different band passes produce different kernels that are sensitive to different volumes of the mesh, thereby contributing unique sampling information to the inversion (e.g., Scire et al., 2016). See Table 2 for details on model space and input data vector.

Using the damped LSQR algorithm of Paige and Saunders (1982), we iteratively inverted our vector of optimized traveltime residuals for a slowness perturbation vector, which was converted back to velocity and plotted as our model. The final model reflects the damping and station/event correction parameters that regularized the inversion to optimize a trade-off between model length and model misfit (Figure S2; e.g., Tikhonov, 1963). Generally, an ideal combination of inversion parameters will suppress the effects of noise and errors in the inversion without obfuscating real structures. This inversion procedure produces the relative velocity perturbation model that best explains our data vector. However, it also simplifies nonlinear model-data relationships such as three-dimensional raypaths and full broadband kernel sensitivity.

To assess the resolution of our model, we conducted synthetic recovery tests using standard checkerboard inputs (e.g., Schmandt & Humphreys, 2010; Van Der Hilst & Mann, 1994; Figure 4) as well as high velocity structures meant to replicate subducting slabs (e.g., Bezada et al., 2010; Widiyantoro & van der Hilst, 1997; Figures 5 and S3). The procedure of these tests is similar to the initial inversion, although it involves an extra forward calculation. First, a known velocity model is multiplied by the sampling/resolution matrix used in the inversion (i.e., the sensitivity kernels), which produces a synthetic data vector. Next, random Gaussian noise is added to the synthetic data and this data vector and the resolution matrix are inverted to obtain a recovered synthetic velocity model using the same LSQR procedure and parameters as the initial inversion. For our synthetic tests, we add 5% standard Gaussian noise (μ = 0 s, σ = 1 s) to each delay in the data vector. Thus, the input and recovered synthetic models can be compared to qualitatively assess the resolving power of the resolution matrix itself. Synthetic tests are a valuable tool to evaluate model resolution, although they do overestimate the resolving power of the model. This stems from the assumption that incomplete data coverage accounts for all uncertainties in the synthetic tests. Nevertheless, qualitatively good visual agreement between the input and output synthetic models suggests that features roughly the same size of or larger than the synthetic pattern can be interpreted. To further evaluate the reliability of our model, we plotted quantitative measurements of the per-voxel sampling density (e.g., Widiyantoro & van der Hilst, 1997; Figure S4).

Table 2
Physical Dimensions of the Mesh Used for Inversion

Axis	Minimum	Maximum	Nodes	Spacing
Depth	0 km	1,000 km	65	~15 km
Latitude	7.5°N	20.5°N	33	~43 km
Longitude	286.5°E	301°E	33	~48 km

4. Results

4.1. Key Features

In the southwestern region of the model a high-velocity feature appears to dip south-southeast beneath northern Venezuela (labeled SC in Figures 6

10.1029/2018GC007603

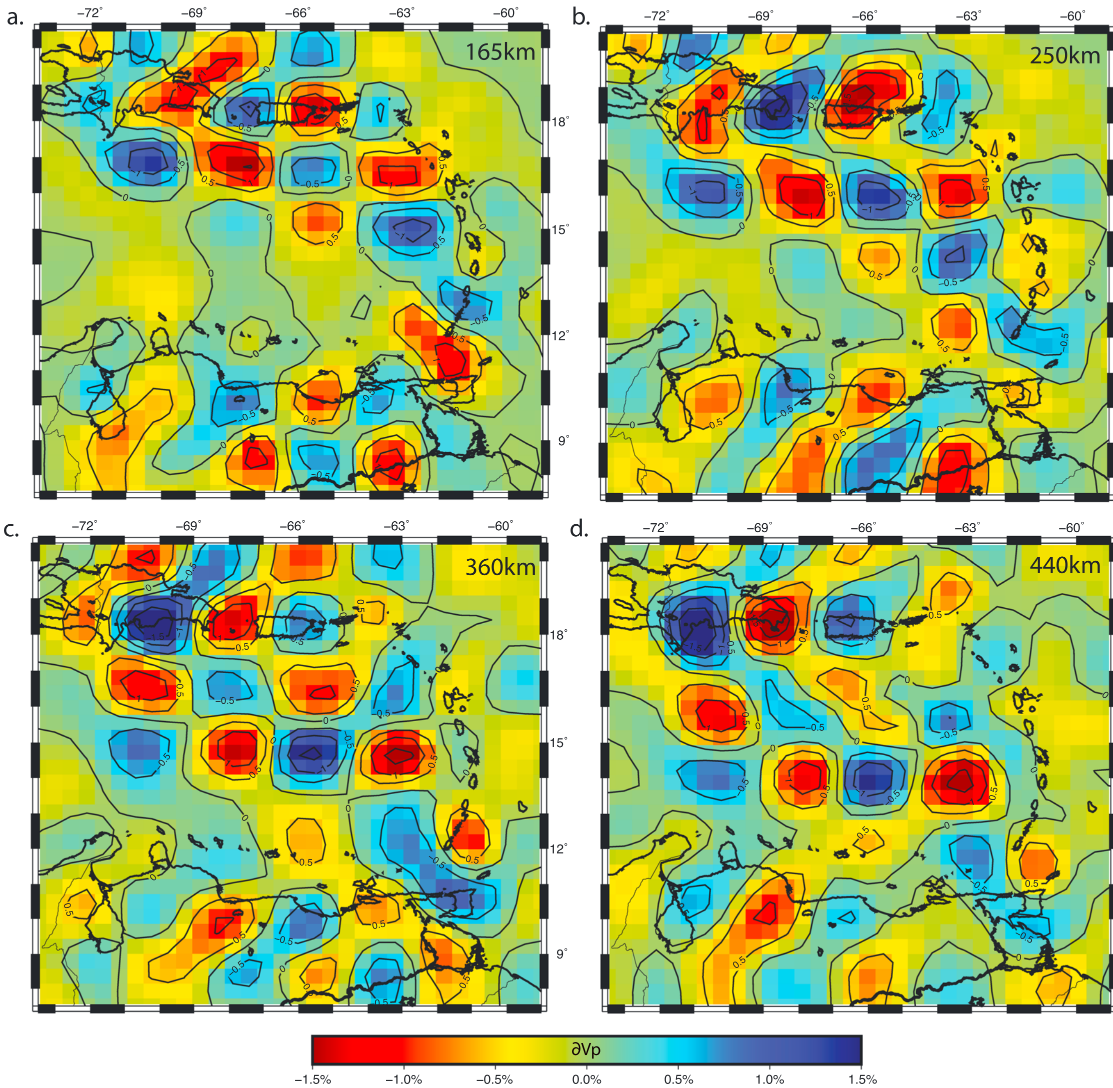

Figure 4. Depth slices of the synthetic checkerboard test. The input checkerboard pattern consists of boxes that alternate between ±4% ∂Vp in each direction and span four voxels in latitude, four voxels in longitude, and eight voxels in depth each. Recovered anomalies are plotted.

and 7). The feature is imaged from shallow depths (≤50 km) down to depths of ~600 km (Figure 7). It is visibly separate from other fast anomalies in the model and extends from north of Lake Maracaibo (~11°N; Figure 1) to the southern edge of the model (7.5°N).

In the southeast region of our model, near the island of Trinidad (Figure 1), we image a steeply west dipping high velocity anomaly (SLA in Figures 6 and 7). Around 10°N, this feature is nearly vertical and extends from shallow depths below the SLA to ~800 km depth beneath northeastern Venezuela (Figure 7). This fast anomaly appears to strike to the northeast and its northern extent has a shallower dip (~70°) beneath the central Lesser Antilles, where it appears to extend to depths of ~700 km (Figure 7). Around 14°–15°N, there is a lateral gap in this fast velocity feature that extends down to a depth of ~200 km, below which it is continuous (Figure 6). Further north, this feature bends around the northern Lesser Antilles where it dips with an angle of $<60°$ to the southeast (Figure 7). In the vicinity of Puerto Rico, the fast, arcuate feature dips moderately steeply (~70°) to the south to a depth of ~750 km (Figure 8). Further west, roughly between Puerto Rico and Hispaniola, there is a narrow discontinuity in the arcuate high-velocity anomaly above a depth of ~300 km, below which it is continuous (Figure 6). West of this gap in the fast velocity anomaly, the feature dips nearly vertically to the south to depths of ~700 km (Figure 8). Overall, the arcuate

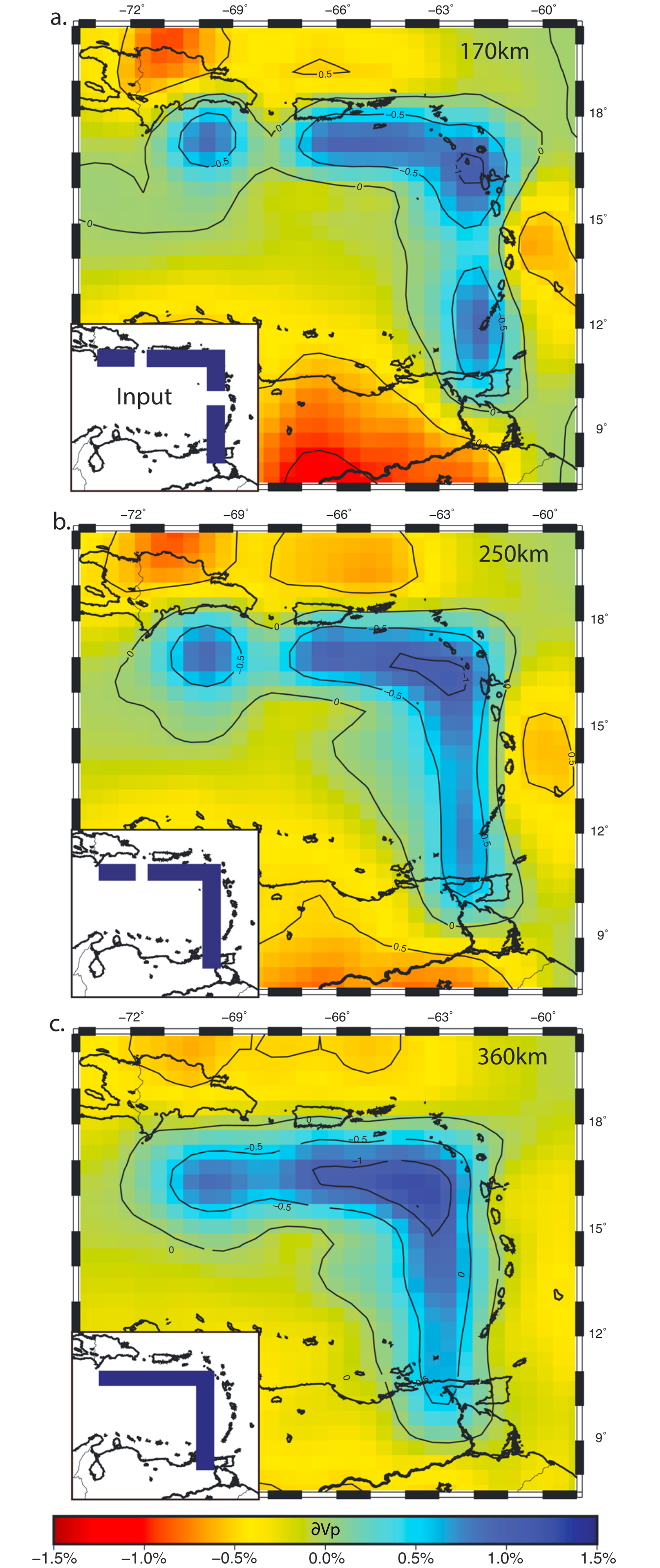

Figure 5. Depth slices of arcuate synthetic slab test. An input pattern consisting of a simple arcuate slab (~125 km thick) with two along-strike discontinuities was solved for. Input anomalies were +4% ∂Vp. Recovered amplitudes are plotted with the input pattern for that depth displayed as insets.

high-velocity feature spans the Lesser and Greater Antilles arcs and forms a spoon-shaped feature with steep cusps and a more gently dipping middle section.

4.2. Resolution Tests

We performed two types of resolution tests: synthetic recoveries and sampling visualization. For the first synthetic recovery test, we conducted a checkerboard test (Figure 4). The input checkerboard pattern consists of boxes that alternate between ±4% ∂Vp in each direction and span four voxels in latitude, four voxels in longitude, and eight voxels in depth each. For the second synthetic test, we inverted an arcuate slab (~125 km thick, +4% ∂Vp) with two main segments: (1) a north-south striking, west dipping slab that spans the Lesser Antilles arc and has a gap in fast material from 14°–15°N above 200 km and (2) an east-west striking, south dipping slab that spans the Greater Antilles and has a gap in fast material from 68.5°−69°W above 300 km (Figure 5). Finally, for the third synthetic test, we inverted a north-south striking, west dipping slab (~125 km thick, +4% ∂Vp) that flattens in the transition zone (410–660 km; Figure S3). To visualize model sampling, we measured data density, plotted as both total ray-length per voxel and absolute value of kernel sensitivity per voxel (Figure S4).

The checkerboard test demonstrates that resolution varies both with depth and raypath coverage (Figure 4). Overall, the main features we discuss below are well recovered, although resolution at shallower depths is restricted to areas underlying dense station spacing. Deeper resolution is more laterally extensive, which reflects the sampling inherent to a wide-aperture array. The second test, using the segmented arcuate slab, was well recovered (Figure 5). This test shows that the inversion preserved, with good fidelity, the extent of the slab along-strike, the arcuate shape of the slab, the two along-strike gaps at shallower depths, and lateral continuity at higher depths. The third test, using the slab flattened in the transition zone, was also well recovered and demonstrates minimal smearing both vertically and horizontally (Figure S3). Slices taken above and below the slab in the transition zone are not highly contaminated by the nearby fast structure either above or below. Finally, the sampling visualization corroborates the observation that the arcuate nature of the array had an effect on the spatial distribution of data constraints (Figure S4). At shallower depths, only areas of the mesh underlying seismometers are well sampled. At greater depths, the middle of the mesh is sampled more densely than the edges. These tests suggest that our model possesses sufficient resolving power, although the synthetic tests do have inherent limitations, which are discussed above.

5. Interpretations

We interpret the fast anomaly beneath northwest Venezuela as subducted Caribbean oceanic lithosphere and the arcuate high-velocity anomalies beneath the Caribbean plate as subducted oceanic lithosphere corresponding to the American plates and the Atlantic. We describe the subducted Atlantic lithosphere as a segmented spoon-shaped slab, which we divide into three sections (starting counterclockwise from the southeast): the SLA, the northern Lesser Antilles, and the Hispaniola fragment.

10.1029/2018GC007603

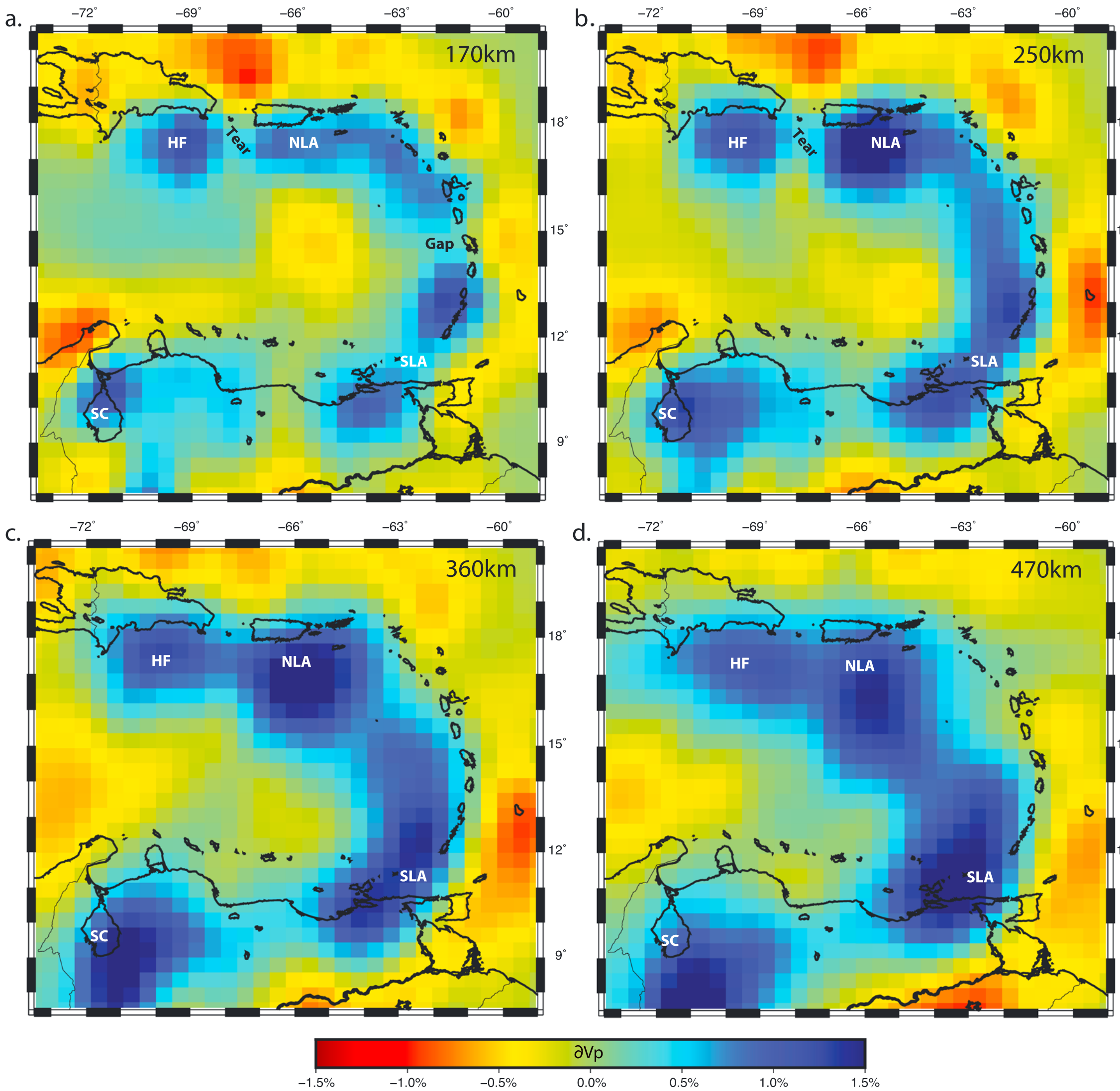

Figure 6. Plan view depth slices of the *P* wave tomographic model. Slices are taken at the depth value displayed in the upper right-hand corner of each panel. Relative *P* wave velocity perturbations are plotted per the color scale beneath the figure. Coastlines are plotted for visual reference. High velocity features are labeled in white font: HF = Hispaniola fragment; NLA = northern Lesser Antilles slab; SLA = southern Lesser Antilles slab; SC = Southern Caribbean lithosphere. Discontinuities in the overall Lesser Antilles slab are labeled in black. We interpret the lateral discontinuities between SLA and NLA as the subducted North American-South American plate boundary and between NLA HF as a slab segmentation tear, respectively.

5.1. Southern Caribbean Anomaly

The Southern Caribbean anomaly we observe is consistent with the previous *P* wave tomographic models of Bezada et al. (2010) and van Benthem et al. (2013). However, the Caribbean slab anomaly we image does not extend as far west as that of the global model (van Benthem et al., 2013) and is more continuous at depths above 300 km than the same feature imaged in the regional model (Bezada et al., 2010). Compared to the regional tomographic model of van der Hilst and Mann (1994), our model shows a steeper, deeper Caribbean slab. The surface wave tomographic model of Miller et al. (2009) also detected the Caribbean beneath Maracaibo, though the underthrust lithosphere was less extensive than what we image due to the methodology and model space.

5.2. Arcuate Slab

Beginning with the SLA slab, we note that there is a dramatic change in slab dip along the strike of the arc. The southern edge of the slab has a nearly vertical dip, which reduces northward toward the middle of the

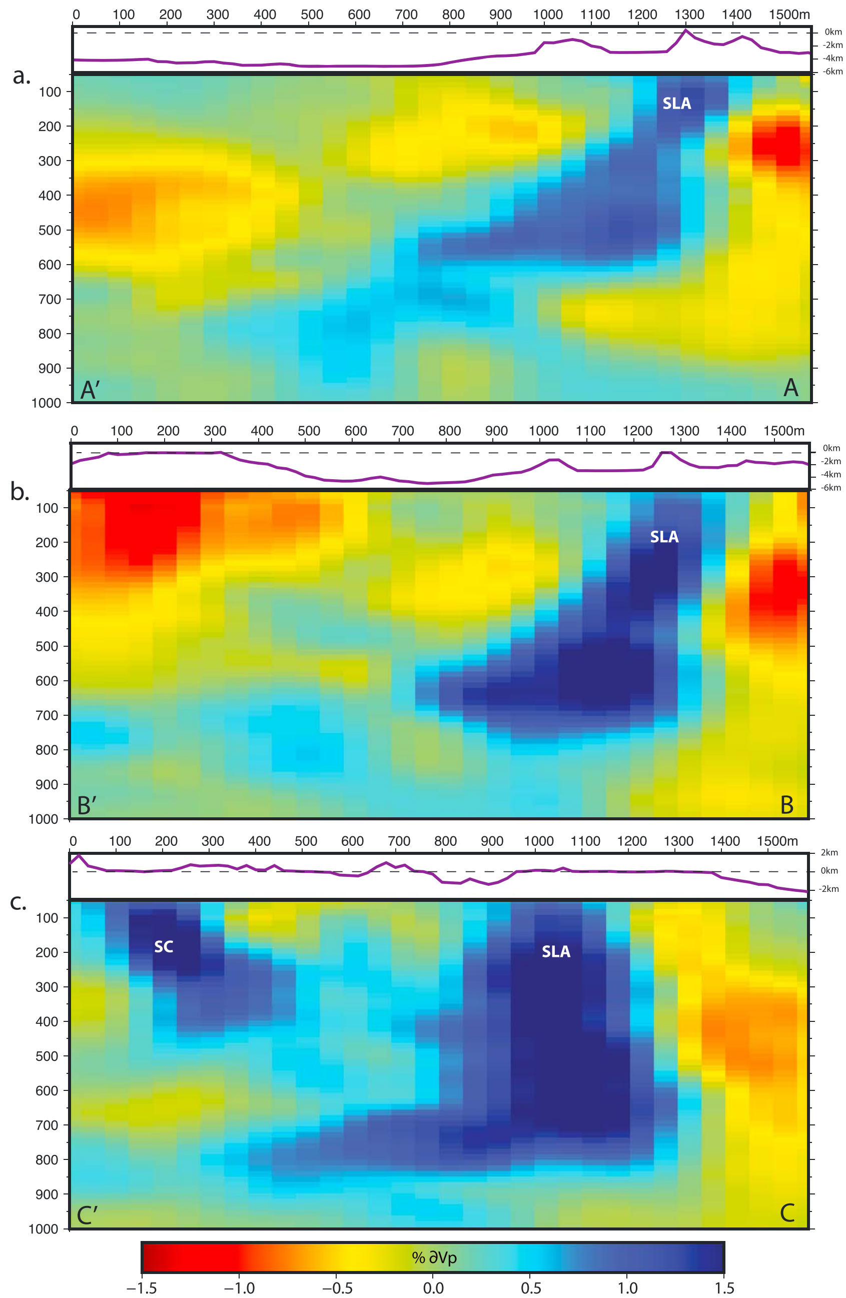

Figure 7. Vertical latitudinal cross sections through the tomographic model. Slices are taken along the transects shown in Figure 2 corresponding to the letters in the bottom corners of each panel. Color scales and key features labeled in white are the same as Figure 6. Topography/bathymetry is plotted above each cross-section.

arc, approximately near the eastern edge of the Puerto Rico microplate, where the slab dip is $<60°$ (Figures 7 and 8). Further west along the curved trench, slab dip steepens before becoming nearly vertical again near eastern Hispaniola. Overall, this appears as a spoon-shaped slab with steep cusps.

The SLA anomaly of our model is consistent with previous body wave tomographic studies. VanDecar et al. (2003) also resolved a steeply dipping SLA slab that extends beyond the deepest regional Wadati-Benioff zone seismicity (~200 km; Figure 2). Bezada et al. (2010) also imaged a nearly vertical slab beneath the SLA, although this feature in their model does not extend south of ~10°N in map-view, compared to ~9°N in our model. The SLA slab in the model of van Benthem et al. (2013) is similar to what we image, as both features dip steeply, have similar extents in map view, and extend to depths of ~800 km.

10.1029/2018GC007603

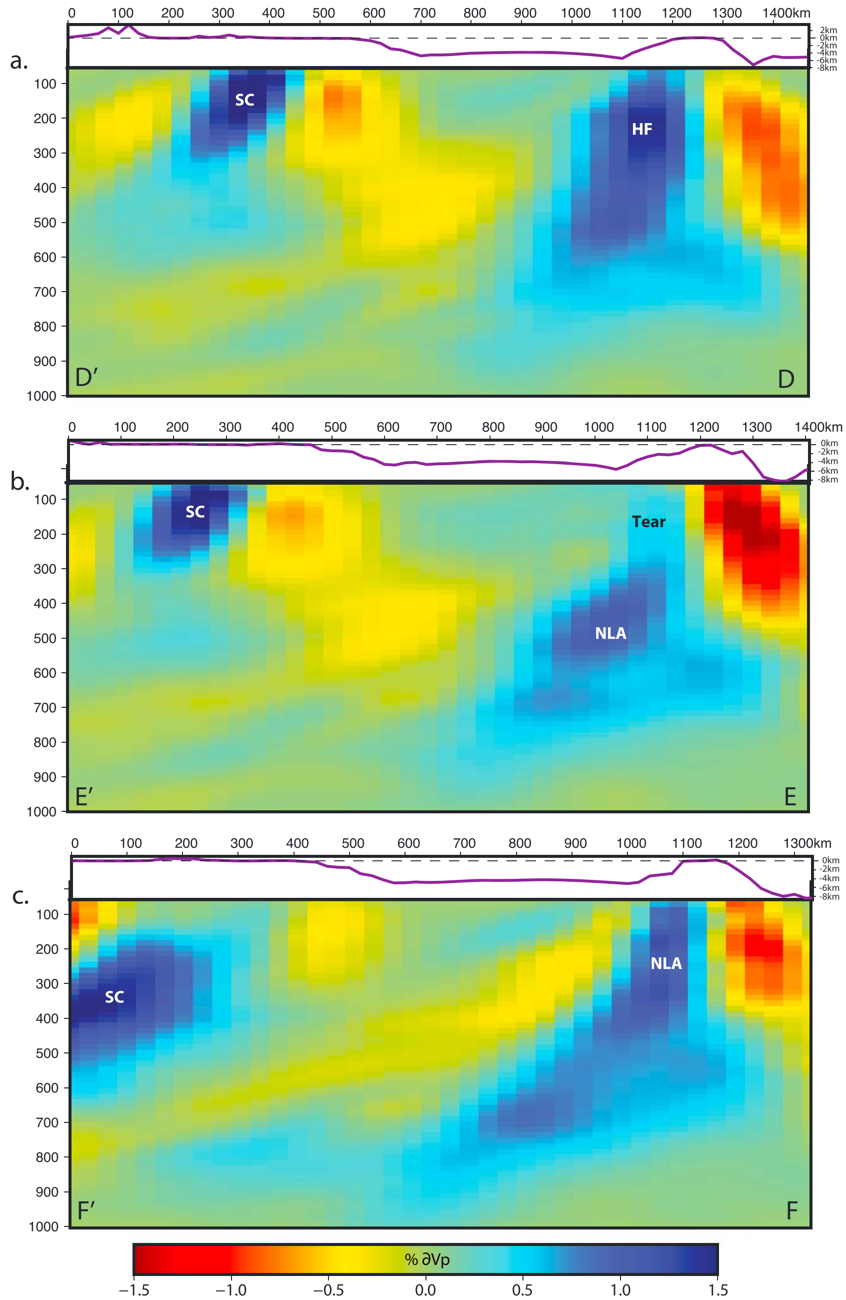

Figure 8. Vertical oblique cross sections through the tomographic model. Slices are taken along the transects in Figure 2 corresponding to the letters in the bottom corners of each panel. Color scales and key features labeled in white are the same as Figure 6. Topography/bathymetry is plotted above each cross-section.

5.3. NA-SA Slab Gap

We image a gap between the southern and northern Lesser Antilles features above ~200 km (Figure 6). We believe this discontinuity corresponds to the boundary between the subducting North and South American plates. This is consistent with the notion of a North American-South American transform plate boundary which extends from the 15–20 fracture zones at the Mid-Atlantic Ridge to the Barracuda Ridge, which subducts beneath the Lesser Antilles arc (e.g., Gordon, 1998; Roest & Collette, 1986). These results agree with previous studies that have divided the Lesser Antilles arc into northern and southern sections near ~15°N due to an abrupt transition from the smooth and deep Grenada basin to the rough and shallow bathymetry further north (Figure 2; Aitken et al., 2011; Schubert & Laredo, 1984), a change in slab dip and arc-to-slab depth (Syracuse & Abers, 2006), and an imaged low velocity zone that separates lengths of high velocity slab (van Benthem et al., 2013).

Of the previous models discussed, only the *P* wave model of van Benthem et al. (2013) extends to the Northern Lesser Antilles and Greater Antilles, thus offering the only comparison in those regions. This model also resolves a gap between the southern and northern Lesser Antilles anomalies, although the two slabs do not appear to merge below 200 km. We attribute this disagreement to differences in the inversion technique and resolution between the global model, of which the Caribbean is a subset, and the present regional study.

5.4. Greater Antilles Slab Gap

We image a gap in the subducting North American oceanic lithosphere between the islands of Puerto Rico and Hispaniola (Figures 6 and 8). This discontinuity underlies the extensional Mona Passage (Figure 1) and extends down to a depth of ~300 km. This slab gap is located downdip from the boundary between the Puerto Rico and Hispaniola microplates and is ~100 km wide. The gap separates the steeply dipping edge of the northern slab from the more gently dipping slab beneath Puerto Rico and the northern Lesser Antilles islands. The gap is visible in map view (Figure 6) and dip-parallel cross sections (Figure 8).

Unlike other features of our model, discussed above, this discontinuity has not been imaged by previous tomographic studies in the region. The global model of van Benthem et al. (2013) includes the Greater Antilles; however, the northern Lesser Antilles anomaly is laterally continuous across the Mona Passage. As with other discrepancies between our model and that of van Benthem et al. (2013), we note that the two models were constructed using different techniques and data sets and that some areas are better resolved in one model than the other.

6. Discussion

6.1. Gradient in Slab Dip

We image an arcuate slab beneath the eastern Caribbean that as a high-velocity anomaly that is continuous at depth and exhibits high slab dip at the ends of the arc and dramatically lower dip angles beneath the middle portion of the arc (Figure 7). Numerical modeling results have related steeper slab dip to the subduction of buoyant material that initiates arc-continent collision (Royden & Husson, 2009). This suggests that observations of steep slab dip along the Lesser Antilles arc may correlate to known collisions. The northern edge of the slab is proximal to the Eocene collision between the former Great Arc of the Caribbean and the Bahamas Plateau (e.g., Pindell & Kennan, 2009). The southern edge of the slab is proximal to the collision between the Caribbean and South America along the South Caribbean Deformed Belt that has been progressing for most of the Cenozoic (e.g., Avé Lallemant, 1997; Escalona & Mann, 2011).

The morphology of the Lesser Antilles slab in our model is consistent with observations of trench retreat and rollback as well. The middle section of the arc, where we observe the shallowest dip angles, has been experiencing slab rollback and back-arc spreading since the Bahamas collision ~55 Ma, (Pindell & Kennan, 2009). This rollback has driven the opening of the Grenada Basin that separates the extinct Aves Ridge from the active Lesser Antilles arc (Aitken et al., 2011). Rollback has also been inferred from observations of seismic anisotropy. When slabs rollback, they induce anisotropic olivine in the subslab upper mantle to align such that the crystallographic fast axis is oriented parallel to the trench (e.g., Long & Becker, 2010). Shear wave splitting studies in the eastern Caribbean reveal a trench-parallel mantle flow pattern beneath Puerto Rico and the Lesser Antilles, which imply a Lesser Antilles slab that is rolling back towards the Atlantic Ocean (Hodges & Miller, 2015; Lynner & Long, 2013; Meighan & Pulliam, 2013; Piñero-Feliciangeli & Kendall, 2008). Given that slab rollback is associated with a reduction in slab dip (e.g., Griffiths et al., 1995; Holt et al., 2015; Royden, 1993), the observed shallower dip in the middle section of the slab, where the most rollback has occurred, can be expected.

6.2. Slab Segmentation in the Greater Antilles

Seismicity near the Puerto Rico Trench as well as seafloor imaging has been used to infer slab fragmentation due to collision and trans-tensional faulting from the corner of the northern Lesser Antilles to Hispaniola

10.1029/2018GC007603

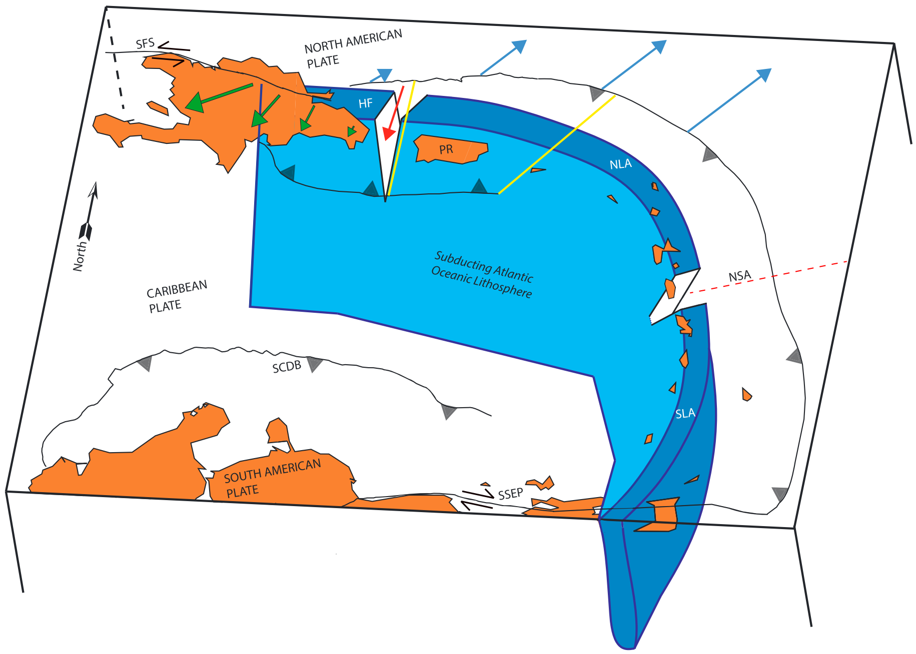

Figure 9. Schematic to illustrate tearing and segmentation of the Atlantic oceanic lithosphere subducting beneath the Lesser and Greater Antilles arcs. Labels are the same as in Figure 1. The downdip segmentation tear between Puerto Rico and Hispaniola is indicated with a red arrow. The NSA plate boundary imaged by this study is extended east of the arc based on Gordon (1998). The green arrows are simplified GPS velocities of Hispaniola with respect to a stable Caribbean plate from Symithe et al. (2015). The blue arrows depict differential trench retreat along the Greater Antilles and northern Lesser Antilles as inferred from the slab dip imaged in this study and previous studies on regional GPS velocities (Symithe et al., 2015) and tectonic reconstructions (Boschman et al., 2014). The yellow lines are simplified boundaries of the Puerto Rico microplate from Byrne et al. (1985).

(Dillon et al., 1996). This would suggest a series of trench-normal tears in the downgoing slab. While our model resolves only one such tear, a separate, downdip tear northeast of Puerto Rico has been inferred through analysis of regional focal mechanisms and stress inversion (Meighan et al., 2013), observations of localized trench-normal mantle flow from shear wave splitting (Schlaphorst et al., 2017), and kinematic reconstructions of rapid uplift of sections of the Puerto Rico trench (ten Brink, 2005). Additionally, the Puerto Rico microplate is migrating ENE relative to a stable North America and undergoing trench-retreat, whereas the Hispaniola plate is progressively coupling to the North American plate (Symithe et al., 2015).

We infer that a slab tear is located beneath the Mona Passage (Figure 9). The Mona Passage is an extensional feature related to oblique subduction and collision with the Bahamas along the northern Caribbean plate boundary (Chaytor & ten Brink, 2010; Mondziel et al., 2010). Extension in this region has also been linked to the pull-away of the North American plate from the edge of the slab beneath Puerto Rico (Speed & Larue, 1991). The Mona Passage has elevated rates of shallow seismicity (e.g., Chaytor & ten Brink, 2010; Molnar & Sykes, 1969), compared to a near absence of intermediate-depth earthquakes (e.g., Masson & Scanlon, 1991). This imbalance has been used as an argument for a local tear or detachment in the slab underlying Puerto Rico (Dolan et al., 1998; Figure 2). A tear here could help explain seismicity in addition to providing a mechanism to accommodate the along-strike transition from steep slab dip near Hispaniola to more gradual slab dip near the northern Lesser Antilles (van Benthem et al., 2013; Figure 8). Furthermore, the formation of the tear could be linked to slab segmentation (e.g., Doglioni, 1991).

Given these observations, we suggest that differential rollback between a retreating Puerto Rico and relatively locked Hispaniola, combined with extensional weakening driven by the opening of the Mona Passage, is producing the tear we image in our model. The tear beneath Mona Passage and the tear east of Puerto Rico suggest a system of trench-normal, downdip tears similar to what has been observed in other segmented arcuate subduction zones such as in the Mediterranean (Rosenbaum et al., 2008).

10.1029/2018GC007603

6.3. Differential Rollback Driving Regional Deformation

Hispaniola and Puerto Rico microplates were originally part of the Caribbean plate, before being detached in the Eocene (Mann et al., 1995). Currently, these two microplates are diverging from one another as independent blocks (Benford et al., 2012). Hispaniola is progressively transferring onto the North American plate (DeMets & Wiggins-Grandison, 2007) while Puerto Rico and the Caribbean Plate migrate northeast relative to a stable North America (Jansma et al., 2000). As Puerto Rico migrates toward the Atlantic, it also rotates, suggesting that it is decoupled from surrounding plates (e.g., Boschman et al., 2014; Reid et al., 1991). Previous studies have documented regional divergence and broadly distributed deformation without invoking a tear that would make such plate motions possible (Benford et al., 2012; van Benthem et al., 2014).

Numerical modeling studies have successfully used distinct tectonic blocks to recreate regional kinematics (Symithe et al., 2015; van Benthem et al., 2014). Collision in the Bahamas and *push* by the westward migrating edge of the North American slab (west of the Mona Passage) have been suggested as the main driving forces for deformation among the tectonic blocks (van Benthem et al., 2014). While these models describe the surface kinematics of the region, captured in plate motions, they lack explanation of related deformation processes in the upper mantle.

We propose that slab rollback is a significant component to regional deformation in the Greater Antilles region and submit the segmentation tear developing between Puerto Rico and Hispaniola as structural evidence. Rollback and trench retreat could explain regional extension, localized zones of deformation, and large-scale rotation (e.g., Faccenna et al., 2004), where such deformation could lead to downdip tearing. Our images alone cannot resolve the origin of the differential rollback, but along-strike changes in slab dip observed in this study, combined with reconstruction efforts (e.g., Pindell & Kennan, 2009), and the relationship between collision and rollback (e.g., Royden, 1993) indicates the Eocene collision between the Bahamas Plateau and the former subduction zone as a potential cause.

6.4. Microplates Facilitating Slab Segmentation

Lithospheric tearing in the SLA is accomplished by one STEP fault at the southern end of the subduction zone, where the slab has a nearly vertical dip. This contrasts with the multiple tears in the Greater Antilles, where the slab has a reduced dip (~60°). These differences may be related to the location of slab tears in the Greater Antilles, which are near microplates. Contrastingly, the tear at the southern edge of the Lesser Antilles slab is bounded by the South American continent. The segmentation tears identified by this study and by Meighan et al. (2013) roughly correspond to the eastern and western boundaries of the Puerto Rico microplate. The tears also coincide with the boundaries of the zone of seismic quiescence (Figure 2; Dolan et al., 1998). We suggest that these tears have developed at the edges of the Puerto Rico microplate as the microplate facilitates differential rollback and regional divergence among discrete tectonic blocks.

In support of this theory, microplate formation and capture have been linked to regional extension in several settings. For example, off the coast of California, a trans-tensional zone is observed above the edge of the Monterey microplate (Nicholson et al., 1994). In the Mediterranean, differential slab rollback between the subducting Tyrrhenian and Ionian microplates has been related to extension in the overriding plate and slab decoupling, suggesting that the presence of distinct blocks along a subduction interface can facilitate deformation and tearing (Gvirtzman & Nur, 1999). Near western Mexico, differential rollback in the presence of small tectonic plates has been observed tomographically, where the Rivera (formerly part of the Cocos) and Cocos plates subduct and diverge at depth due to recent rollback of the Rivera slab (Yang et al., 2009).

Changes in subduction geometry are related to the deformation of lithosphere that has already subducted. Conceptually, an upper plate composed of discrete blocks should allow for the geometry of subduction and convergence to vary as a function of divergence among the blocks. The proposed role of microplates facilitating slab segmentation helps explain the presence of microplates near several observed tears and invites the search for more tears near other subduction zones that feature microplates.

7. Conclusions

We inverted a data set of ~20,000 optimized traveltime residuals of *P* and *PP* arrivals recorded across a regional network of broadband seismometers to construct a relative velocity model for the eastern Caribbean upper mantle. This model reveals an arcuate slab corresponding to North and South American oceanic lithosphere that has subducted beneath the Caribbean, as well as southern Caribbean lithosphere that has subducted beneath northern South America. We identify two along-strike discontinuities in the Antilles slab, which we relate to the North America-South America plate boundary and a segmentation tear between the Puerto Rico and Hispaniola microplates. We suggest that this slab tear implies differential rollback near the northern Lesser Antilles. This hypothesis helps explain various geodetic observations and numerical modeling results that have identified anomalous plate motions in the northeastern Caribbean but have not reached a consensus as to what drives regional deformation and how this deformation is accommodated at depth. We suggest that the presence of microplates enables block divergence, extension, and thereby differential rollback and slab segmentation. Thus, the contrast in tearing/deformation style between the northern and southern limbs of the Antilles subduction system may relate to the presence of microplates.

Acknowledgments
This work was supported by NSF CAREER grant EAR-1054638. Data were shared by the Seismic Research Centre at the University of the West Indies and Incorporated Research Institutions for Seismology (IRIS). Data from IRIS are available online through the IRIS data management center (DMC). Special thanks are given to Joan L. Latchman and Richard Robertson (University of the West Indies Seismic Research Centre) for access to data and help in preparing this manuscript. Figures were made with Generic Mapping Tools (Wessel et al., 2013).

References

Aitken, T., Mann, P., Escalona, A., & Christeson, G. L. (2011). Evolution of the Grenada and Tobago basins and implications for arc migration. *Marine and Petroleum Geology*, *28*(1), 235–258. https://doi.org/10.1016/j.marpetgeo.2009.10.003

Aki, K., Christoffersson, A., & Husebye, E. S. (1977). Determination of the three-dimensional seismic structure of the lithosphere. *Journal of Geophysical Research*, *82*(2), 277–296. https://doi.org/10.1029/JB082i002p00277

Avé Lallemant, H. G. (1997). Transpression, displacement partitioning, and exhumation in the eastern Caribbean/South American plate boundary zone. *Tectonics*, *16*(2), 272–289. https://doi.org/10.1029/96TC03725

Benford, B., DeMets, C., & Calais, E. (2012). GPS estimates of microplate motions, northern Caribbean: Evidence for a Hispaniola microplate and implications for earthquake hazard. *Geophysical Journal International*, *191*(2), 481–490. https://doi.org/10.1111/j.1365-246X.2012.05662.x

Bezada, M. J., Levander, A., & Schmandt, B. (2010). Subduction in the southern Caribbean: Images from finite-frequency *P* wave tomography. *Journal of Geophysical Research*, *115*, B12333. https://doi.org/10.1029/2010JB007682

Bijwaard, H., Spakman, W., & Engdahl, E. R. (1998). Closing the gap between regional and global travel time tomography. *Journal of Geophysical Research*, *103*(B12), 30,055–30,078. https://doi.org/10.1029/98JB02467

Bird, P. (2003). An updated digital model of plate boundaries. *Geochemistry, Geophysics, Geosystems*, *4*(3), 1027. https://doi.org/10.1029/2001GC000252

Boschman, L. M., van Hinsbergen, D. J., Torsvik, T. H., & Spakman, W. (2014). Kinematic reconstruction of the Caribbean region since the Early Jurassic. *Earth-Science Reviews*, *138*, 102.

Burke, K. (1988). Tectonic evolution of the Caribbean. *Annual Review of Earth and Planetary Sciences*, *16*(1), 201–230. https://doi.org/10.1146/annurev.ea.16.050188.001221

Byrne, D. B., Suarez, G., & McCann, W. R. (1985). Muertos trough subduction—Microplate tectonics in the northern Caribbean? *Nature*, *317*(6036), 420. https://doi.org/10.1038/317420a0

Calais, E., Béthoux, N., & de Lépinay, B. M. (1992). From transcurrent faulting to frontal subduction: A seismotectonic study of the northern Caribbean plate boundary from Cuba to Puerto Rico. *Tectonics*, *11*(1), 114–123. https://doi.org/10.1029/91TC02364

Chaytor, J. D., & ten Brink, U. S. (2010). Extension in Mona Passage, Northeast Caribbean. *Tectonophysics*, *493*(1), 74–92. https://doi.org/10.1016/j.tecto.2010.07.002

Clark, S. A., Sobiesiak, M., Zelt, C. A., & Magnani, M. B. (2008). Identification and tectonic implications of a tear in the South American plate at the southern end of the Lesser Antilles. *Geochemistry, Geophysics, Geosystems*, *9*, Q11004. https://doi.org/10.1029/2008GC002084

Dahlen, F. A., Hung, S.-H., & Nolet, G. (2000). Fréchet kernels for finite-frequency traveltimes—I. Theory. *Geophysical Journal International*, *141*(1), 157–174. https://doi.org/10.1046/j.1365-246X.2000.00070.x

DeMets, C., & Wiggins-Grandison, M. (2007). Deformation of Jamaica and motion of the Gonâve microplate from GPS and seismic data. *Geophysical Journal International*, *168*(1), 362–378. https://doi.org/10.1111/j.1365-246X.2006.03236.x

Dillon, W. P., Edgar, N. T., Scanlon, K. M., & Coleman, D. F. (1996). A review of the tectonic problems of the strike-slip northern boundary of the Caribbean plate and examination by GLORIA. Geology of the United States' Seafloor: The View From GLORIA, 135–164.

Doglioni, C. (1991). A proposal for the kinematic modelling of W-dipping subductions-possible applications to the Tyrrhenian-Apennines system. *Terra Nova*, *3*(4), 423–434. https://doi.org/10.1111/j.1365-3121.1991.tb00172.x

Doglioni, C. (1995). Geological remarks on the relationships between extension and convergent geodynamic settings. *Tectonophysics*, *252*(1–4), 253–267.

Doglioni, C., Mongelli, F., & Pieri, P. (1994). The Puglia uplift (SE Italy): An anomaly in the foreland of the Apenninic subduction due to buckling of a thick continental lithosphere. *Tectonics*, *13*(5), 1309–1321. https://doi.org/10.1029/94TC01501

Dolan, J. F., Mullins, H. T., & Wald, D. J. (1998). Active tectonics of the north-central Caribbean: Oblique collision, strain partitioning, and opposing subducted slabs. In Special Paper 326: Active Strike-Slip and Collisional Tectonics of the Northern Caribbean Plate Boundary Zone. *Geological Society of America.*, *326*, 1–61. https://doi.org/10.1130/0-8137-2326-4.1

Dvorkin, J., Nur, A., Mavko, G., & Ben-Avraham, Z. (1993). Narrow subducting slabs and the origin of backarc basins. *Tectonophysics*, *227*(1–4), 63–79.

Escalona, A., & Mann, P. (2011). Tectonics, basin subsidence mechanisms, and paleogeography of the Caribbean-South American plate boundary zone. *Marine and Petroleum Geology*, *28*(1), 8–39. https://doi.org/10.1016/j.marpetgeo.2010.01.016

Faccenna, C., Bellier, O., Martinod, J., Piromallo, C., & Regard, V. (2006). Slab detachment beneath eastern Anatolia: A possible cause for the formation of the North Anatolian fault. *Earth and Planetary Science Letters*, *242*(1), 85–97. https://doi.org/10.1016/j.epsl.2005.11.046

Faccenna, C., Piromallo, C., Crespo-Blanc, A., Jolivet, L., & Rossetti, F. (2004). Lateral slab deformation and the origin of the western Mediterranean arcs. *Tectonics*, *23*, TC1012. https://doi.org/10.1029/2002TC001488

Gordon, R. G. (1998). The plate tectonic approximation: Plate nonrigidity, diffuse plate boundaries, and global plate reconstructions. *Annual Review of Earth and Planetary Sciences*, *26*(1), 615–642.

Govers, R., & Wortel, M. J. R. (2005). Lithosphere tearing at STEP faults: Response to edges of subduction zones. *Earth and Planetary Science Letters*, *236*(1), 505–523. https://doi.org/10.1016/j.epsl.2005.03.022

Granja Bruña, J. L., ten Brink, U. S., Carbó-Gorosabel, A., & Muñoz-Martín, A. (2009). Morphotectonics of the central Muertos thrust belt and Muertos trough (northeastern Caribbean). *Marine Geology*, *263*(1), 7–33. https://doi.org/10.1016/j.margeo.2009.03.010

Griffiths, R. W., Hackney, R. I., & van der Hilst, R. D. (1995). A laboratory investigation of effects of trench migration on the descent of subducted slabs. *Earth and Planetary Science Letters*, *133*(1–2), 1–17.

Gvirtzman, Z., & Nur, A. (1999). The formation of Mount Etna as the consequence of slab rollback. *Nature*, *401*(6755), 782. https://doi.org/10.1038/44555

Hinsbergen, D. J., Vissers, R. L., & Spakman, W. (2014). Origin and consequences of western Mediterranean subduction, rollback, and slab segmentation. *Tectonics*, *33*, 393–419. https://doi.org/10.1002/2013TC003349

Hodges, M., & Miller, M. S. (2015). Mantle flow at the highly arcuate northeast corner of the Lesser Antilles subduction zone: Constraints from shear-wave splitting analyses. *Lithosphere*, *7*(5), 579–587.

Holt, A. F., Becker, T. W., & Buffett, B. A. (2015). Trench migration and overriding plate stress in dynamic subduction models. *Geophysical Journal International*, *201*(1), 172–192.

Humphreys, E., Clayton, R. W., & Hager, B. H. (1984). A tomographic image of mantle structure beneath Southern California. *Geophysical Research Letters*, *11*(7), 625. https://doi.org/10.1029/GL011i007p00625

Hung, S.-H., Dahlen, F. A., & Nolet, G. (2000). Fréchet kernels for finite-frequency traveltimeséII. Examples. *Geophysical Journal International*, *141*(1), 175–203. https://doi.org/10.1046/j.1365-246X.2000.00072.x

Jansma, P. E., Mattioli, G. S., Lopez, A., DeMets, C., Dixon, T. H., Mann, P., & Calais, E. (2000). Neotectonics of Puerto Rico and the Virgin Islands, northeastern Caribbean, from GPS geodesy. *Tectonics*, *19*(6), 1021–1037. https://doi.org/10.1029/1999TC001170

Jolivet, L., Faccenna, C., Huet, B., Labrousse, L., Le Pourhiet, L., Lacombe, O., et al. (2013). Aegean tectonics: Strain localisation, slab tearing and trench retreat. *Tectonophysics*, *597–598*, 1–33. https://doi.org/10.1016/j.tecto.2012.06.011

Kellogg, J. N., & Bonini, W. E. (1982). Subduction of the Caribbean plate and basement uplifts in the overriding South American Plate. *Tectonics*, *1*(3), 251–276. https://doi.org/10.1029/TC001i003p00251

Kennett, B. L. N., & Engdahl, E. R. (1991). Traveltimes for global earthquake location and phase identification. *Geophysical Journal International*, *105*(2), 429–465.

Kumar, P., Srijayanthi, G., & Ravi Kumar, M. (2016). Seismic evidence for tearing in the subducting Indian slab beneath the Andaman arc. *Geophysical Research Letters*, *43*, 4899–4904. https://doi.org/10.1002/2016GL068590

Kundu, B., & Gahalaut, V. K. (2010). An investigation into the seismic potential of the Irrawaddy region, northern Sunda ArcShort note. *Bulletin of the Seismological Society of America*, *100*(2), 891–895. https://doi.org/10.1785/0120090081

Levander, A., Bezada, M. J., Niu, F., Humphreys, E. D., Palomeras, I., Thurner, S. M., et al. (2014). Subduction-driven recycling of continental margin lithosphere. *Nature*, *515*(7526), 253.

Long, M. D., & Becker, T. W. (2010). Mantle dynamics and seismic anisotropy. *Earth and Planetary Science Letters*, *297*(3–4), 341–354.

Lucente, F. P., Chiarabba, C., Cimini, G. B., & Giardini, D. (1999). Tomographic constraints on the geodynamic evolution of the Italian region. *Journal of Geophysical Research*, *104*(B9), 20,307–20,327. https://doi.org/10.1029/1999JB900147

Lynner, C., & Long, M. D. (2013). Sub-slab seismic anisotropy and mantle flow beneath the Caribbean and Scotia subduction zones: Effects of slab morphology and kinematics. *Earth and Planetary Science Letters*, *361*, 367–378.

Mann, P., Calais, E., Ruegg, J.-C., & DeMets, C. (2002). Oblique collision in the northeastern Caribbean from GPS measurements and geological observations. *Tectonics*, *21*(6), 1057. https://doi.org/10.1029/2001TC001304

Mann, P., Schubert, C., & Burke, K. (1990). Review of Caribbean neotectonics, 1990, 307–338.

Mann, P., Taylor, F. W., Edwards, R. L., & Ku, T.-L. (1995). Actively evolving microplate formation by oblique collision and sideways motion along strike-slip faults: An example from the northeastern Caribbean plate margin. *Tectonophysics*, *246*(1), 1–69. https://doi.org/10.1016/0040-1951(94)00268-E

Martinod, J., Funiciello, F., Faccenna, C., Labanieh, S., & Regard, V. (2005). Dynamical effects of subducting ridges: Insights from 3-D laboratory models. *Geophysical Journal International*, *163*(3), 1137–1150.

Masson, D. G., & Scanlon, K. M. (1991). The neotectonic setting of Puerto Rico. *Geological Society of America Bulletin*, *103*(1), 144–154.

Meighan, H. E., & Pulliam, J. (2013). Seismic anisotropy beneath the northeastern Caribbean: Implications for the subducting North American lithosphere. *Bulletin de La Société Géologique de France*, *184*(1–2), 67–76.

Meighan, H. E., Pulliam, J., ten Brink, U., & López-Venegas, A. M. (2013). Seismic evidence for a slab tear at the Puerto Rico Trench. *Journal of Geophysical Research: Solid Earth*, *118*, 2915–2923. https://doi.org/10.1002/jgrb.50227

Meighan, H. E., ten Brink, U., & Pulliam, J. (2013). Slab tears and intermediate-depth seismicity. *Geophysical Research Letters*, *40*, 4244–4248. https://doi.org/10.1002/grl.50830

Millen, D. W., & Hamburger, M. W. (1998). Seismological evidence for tearing of the Pacific plate at the northern termination of the Tonga subduction zone. *Geology*, *26*(7), 659–662.

Miller, M. S., Gorbatov, A., & Kennett, B. L. N. (2006). Three-dimensional visualization of a near-vertical slab tear beneath the southern Mariana arc. *Geochemistry, Geophysics, Geosystems*, *7*, Q06012. https://doi.org/10.1029/2005GC001110

Miller, M. S., Levander, A., Niu, F., & Li, A. (2009). Upper mantle structure beneath the Caribbean-South American plate boundary from surface wave tomography. *Journal of Geophysical Research*, *114*, B01312. https://doi.org/10.1029/2007JB005507

Molnar, P., & Sykes, L. R. (1969). Tectonics of the caribbean and middle america regions from focal mechanisms and seismicity. *Bulletin of the Geological Society of America*, *80*(9), 1639–1684. https://doi.org/10.1130/0016-7606(1969)80(1639:TOTCAM)2.0.CO;2

Mondziel, S., Grindlay, N., Mann, P., Escalona, A., & Abrams, L. (2010). Morphology, structure, and tectonic evolution of the Mona canyon (northern Mona passage) from multibeam bathymetry, side-scan sonar, and seismic reflection profiles. *Tectonics*, *29*, TC2003. https://doi.org/10.1029/2008TC002441

Nicholson, C., Sorlien, C. C., Atwater, T., Crowell, J. C., & Luyendyk, B. P. (1994). Microplate capture, rotation of the western Transverse Ranges, and initiation of the San Andreas transform as a low-angle fault system. *Geology*, *22*(6), 491–495.

Nolet, G. (1987). Seismic wave propagation and seismic tomography. In *Seismic tomography* (pp. 1–23). New York: Springer. Retrieved from http://link.springer.com/content/pdf/10.1007/978-94-009-3899-1_1.pdf

Obrebski, M., Allen, R. M., Pollitz, F., & Hung, S.-H. (2011). Lithosphere–asthenosphere interaction beneath the western United States from the joint inversion of body-wave traveltimes and surface-wave phase velocities. *Geophysical Journal International*, *185*(2), 1003–1021. https://doi.org/10.1111/j.1365-246X.2011.04990.x

Obrebski, M., Allen, R. M., Xue, M., & Hung, S.-H. (2010). Slab-plume interaction beneath the Pacific Northwest. *Geophysical Research Letters*, *37*, L14305. https://doi.org/10.1029/2010GL043489

Paige, C. C., & Saunders, M. A. (1982). LSQR: An algorithm for sparse linear equations and sparse least squares. *ACM Transactions on Mathematical Software*, *8*(1), 43–71.

Perfit, M. R., Heezen, B. C., Rawson, M., & Donnelly, T. W. (1980). Chemistry, origin and tectonic significance of metamorphic rocks from the Puerto Rico Trench. *Marine Geology*, *34*(3), 125–156. https://doi.org/10.1016/0025-3227(80)90069-9

Pindell, J., & Dewey, J. F. (1982). Permo-Triassic reconstruction of western Pangea and the evolution of the Gulf of Mexico/Caribbean region. *Tectonics*, *1*(2), 179–211. https://doi.org/10.1029/TC001i002p00179

Pindell, J. L., & Barrett, S. F. (1991). Geological evolution of the Caribbean region; A plate-tectonic perspective. In G. Dengo & J. E. Case (Eds.), *The Caribbean Region* (pp. 405–432). Guatemala City, Guatemala: Geological Society of America. https://doi.org/10.1130/DNAG-GNA-H.405

Pindell, J. L., & Kennan, L. (2009). Tectonic evolution of the Gulf of Mexico, Caribbean and northern South America in the mantle reference frame: An update. *Geological Society, London, Special Publications*, *328*(1), 1–55. https://doi.org/10.1144/SP328.1

Piñero-Feliciangeli, L. T., & Kendall, J.-M. (2008). Sub-slab mantle flow parallel to the Caribbean plate boundaries: Inferences from SKS splitting. *Tectonophysics*, *462*(1–4), 22–34.

Porritt, R. W., Allen, R. M., & Pollitz, F. F. (2014). Seismic imaging east of the Rocky Mountains with USArray. *Earth and Planetary Science Letters*, *402*, 16–25. https://doi.org/10.1016/j.epsl.2013.10.034

Reid, J. A., Plumley, P. W., & Schellekens, J. H. (1991). Paleomagnetic evidence for Late Miocene counterclockwise rotation of North Coast carbonate sequence, Puerto Rico. *Geophysical Research Letters*, *18*(3), 565–568. https://doi.org/10.1029/91GL00401

Roest, W. R., & Collette, B. J. (1986). The fifteen twenty fracture zone and the North American–South American plate boundary. *Journal of the Geological Society*, *143*(5), 833–843. https://doi.org/10.1144/gsjgs.143.5.0833

Rosenbaum, G., Gasparon, M., Lucente, F. P., Peccerillo, A., & Miller, M. S. (2008). Kinematics of slab tear faults during subduction segmentation and implications for Italian magmatism. *Tectonics*, *27*, TC2008. https://doi.org/10.1029/2007TC002143

Royden, L. H. (1993). Evolution of retreating subduction boundaries formed during continental collision. *Tectonics*, *12*(3), 629–638. https://doi.org/10.1029/92TC02641

Royden, L. H., & Husson, L. (2009). Subduction with variations in slab buoyancy: Models and application to the Banda and Apennine systems. In *Subduction zone geodynamics* (pp. 35–45). Berlin Heidelberg: Springer.

Russo, R. M., Speed, R. C., Okal, E. A., Shepherd, J. B., & Rowley, K. C. (1993). Seismicity and tectonics of the southeastern Caribbean. *Journal of Geophysical Research*, *98*(B8), 14,299–14,319. https://doi.org/10.1029/93JB00507

Sachpazi, M., Laigle, M., Charalampakis, M., Diaz, J., Kissling, E., Gesret, A., et al. (2016). Segmented Hellenic slab rollback driving Aegean deformation and seismicity. *Geophysical Research Letters*, *43*, 651–658. https://doi.org/10.1002/2015GL066818

Sacks, P. E., & Secor, D. T. Jr. (1990). Delamination in collisional orogens. *Geology*, *18*(10), 999–1002.

Schellart, W. P. (2005). Influence of the subducting plate velocity on the geometry of the slab and migration of the subduction hinge. *Earth and Planetary Science Letters*, *231*(3–4), 197–219.

Schlaphorst, D., Kendall, J.-M., Baptie, B., Latchman, J. L., & Tait, S. (2017). Gaps, tears and seismic anisotropy around the subducting slabs of the Antilles. *Tectonophysics*, *698*(Supplement C), 65–78. https://doi.org/10.1016/j.tecto.2017.01.002

Schmandt, B., & Humphreys, E. (2010). Complex subduction and small-scale convection revealed by body-wave tomography of the western United States upper mantle. *Earth and Planetary Science Letters*, *297*(3–4), 435–445. https://doi.org/10.1016/j.epsl.2010.06.047

Schubert, C., & Laredo, M. (1984). Geology of Aves Island (Venezuela) and subsidence of Aves Ridge, Caribbean Sea. *Marine Geology*, *59*(1–4), 305–318.

Scire, A., Zandt, G., Beck, S., Long, M., Wagner, L., Minaya, E., & Tavera, H. (2016). Imaging the transition from flat to normal subduction: Variations in the structure of the Nazca slab and upper mantle under southern Peru and northwestern Bolivia. *Geophysical Journal International*, *204*(1), 457–479.

Silver, E. A., Case, J. E., & Macgillavry, H. J. (1975). Geophysical study of the Venezuelan Borderland. *Geological Society of America Bulletin*, *86*(2), 213–226. https://doi.org/10.1130/0016-7606(1975)86<213:GSOTVB>2.0.CO;2

Spakman, W., & Wortel, R. (2004). A tomographic view on western Mediterranean geodynamics. In *The TRANSMED atlas. The Mediterranean region from crust to mantle* (pp. 31–52). Berlin, Heidelberg: Springer.

Speed, R. C. (1985). Cenozoic collision of the Lesser Antilles Arc and continental South America and the origin of the El Pilar Fault. *Tectonics*, *4*(1), 41–69. https://doi.org/10.1029/TC004i001p00041

Speed, R. C., & Larue, D. K. (1991). Extension and transtension in the plate boundary zone of the northeastern Caribbean. *Geophysical Research Letters*, *18*(3), 573–576. https://doi.org/10.1029/91GL00394

Symithe, S., Calais, E., Chabalier, J. B., Robertson, R., & Higgins, M. (2015). Current block motions and strain accumulation on active faults in the Caribbean. *Journal of Geophysical Research: Solid Earth*, *120*, 3748–3774. https://doi.org/10.1002/2014JB011779

Syracuse, E. M., & Abers, G. A. (2006). Global compilation of variations in slab depth beneath arc volcanoes and implications. *Geochemistry, Geophysics, Geosystems*, *7*, Q05017. https://doi.org/10.1029/2005GC001045

Taboada, A., Rivera, L. A., Fuenzalida, A., Cisternas, A., Philip, H., Bijwaard, H., et al. (2000). Geodynamics of the northern Andes: Subductions and intracontinental deformation (Colombia). *Tectonics*, *19*(5), 787–813. https://doi.org/10.1029/2000TC900004

ten Brink, U. (2005). Vertical motions of the Puerto Rico trench and Puerto Rico and their cause. *Journal of Geophysical Research*, *110*, B06404. https://doi.org/10.1029/2004JB003459

Tikhonov, A. N. (1963). On the solution of ill-posed problems and the method of regularization. *Doklady Akademii Nauk SSSR*, *151*, 501–504.

van Benthem, S., Govers, R., Spakman, W., & Wortel, R. (2013). Tectonic evolution and mantle structure of the Caribbean. *Journal of Geophysical Research: Solid Earth*, *118*, 3019–3036. https://doi.org/10.1002/jgrb.50235

van Benthem, S., Govers, R., & Wortel, R. (2014). What drives microplate motion and deformation in the northeastern Caribbean plate boundary region? *Tectonics*, *33*, 850–873. https://doi.org/10.1002/2013TC003402

Van Der Hilst, R., & Mann, P. (1994). Tectonic implications of tomographic images of subducted lithosphere beneath northwestern South America. *Geology*, *22*(5), 451–454. https://doi.org/10.1130/0091-7613(1994)022<0451:TIOTIO>2.3.CO;2

VanDecar, J. C., & Crosson, R. S. (1990). Determination of teleseismic relative phase arrival times using multi-channel cross-correlation and least squares. *Bulletin of the Seismological Society of America*, *80*(1), 150–169.

VanDecar, J. C., Russo, R. M., James, D. E., Ambeh, W. B., & Franke, M. (2003). Aseismic continuation of the Lesser Antilles slab beneath continental South America. *Journal of Geophysical Research*, *108*(B1), 2043. https://doi.org/10.1029/2001JB000884

Wessel, P., Smith, W. H. F., Scharroo, R., Luis, J. F., & Wobbe, F. (2013). GMT 5: A major new release of the Generic Mapping Tools. *Eos, Transactions of the American Geophysical Union*, *94*(45), 409–410.

Widiyantoro, S., & van der Hilst, R. (1997). Mantle structure beneath Indonesia inferred from high-resolution tomographic imaging. *Geophysical Journal International*, *130*(1), 167–182.

Wortel, M. J. R., & Spakman, W. (2000). Subduction and slab detachment in the Mediterranean-Carpathian region. *Science*, *290*(5498), 1910–1917. https://doi.org/10.1126/science.290.5498.1910

Yang, T., Grand, S. P., Wilson, D., Guzman-Speziale, M., Gomez-Gonzalez, J. M., Dominguez-Reyes, T., & Ni, J. (2009). Seismic structure beneath the Rivera subduction zone from finite-frequency seismic tomography. *Journal of Geophysical Research*, *114*, B01302. https://doi.org/10.1029/2008JB005830

Zhao, L., Jordan, T. H., & Chapman, C. H. (2000). Three-dimensional Fréchet differential kernels for seismicdelay times. *Geophysical Journal International*, *141*(3), 558–576. https://doi.org/10.1046/j.1365-246x.2000.00085.x